Estimation of anticorrosion, antibacterial, and antioxidant activities of a novel compound as an inhibitor for carbon steel in acid media

Nada Ahmed Rasheed Al-qasii, Rawaa Abbas Mohammed, Saba Zuhair Hussein
Department of Chemistry, Collage of Science, University of Baghdad, Jadriyah, Baghdad, 10011, Iraq
E-mail: rawaa.a.mohammed@sc.uobaghdad.edu.iq

The multifunctional properties related to a recently discovered Schiff base compound, [5-(4-nitrophenyl)-4-((4-phenoxybenzylidene)amino)-4H-1,2,4-triazole-3-thiol] (NPAT), as one of the effective corrosion inhibitors for carbon steel in acidic environment are examined in the presented work. Potentiodynamic polarization as well as electro-chemical impedance spectroscopy approaches have been utilized to assess the compound's anticorrosive efficacy. In addition, its antibacterial and antioxidant properties were assessed using disc diffusion and DPPH methods, respectively. Results showed significant inhibition efficiency, particularly at optimal concentrations, as well as notable biological activities, highlighting the compound's potential in industrial and biological applications.

INTRODUCTION

Metal structure deterioration due to interactions with the environment is known as corrosion [1-3]. This process, which often entails the oxidation of metals, causes the material's characteristics to deteriorate due to electrochemical or chemical process with the environment [4, 5]. This issue has been observed in the use of alloys. Metal and alloy assemblies could suffer severe damage from corrosion, which might lead to financial consequences related to replacement, restoration, protection, product waste, and environmental contamination [6, 7]. According to studies, rust is the cause of over 45 % of steel manufacturing breakdowns [8]. Corrosion is a major global economic concern, regardless of whether it is caused by electrochemical or chemical interactions [9, 10]. Steel alloys are utilized in many different fields, such as construction and design, and are subjected to a range of conditions, such as aggressive solutions [11-13]. For instance, acidic solutions are quite corrosive and seriously harm metallic structures. To extend alloys and metallic lifespan, there are many strategies to prevent corrosion and its rate of spread. These techniques include corrosion inhibitors, coatings, cathodic and anodic defense, material design, and selection [14, 15]. But of all such methods, using corrosion protectors is generally favored as a result of its low cost and ease of use [16, 17]. Thus, it was extensively studied and advised to employ corrosion inhibitors to control the deterioration regarding such inexpensive and necessary engineering material in the case when it comes into contact with corrosive media and environmental conditions [18, 19]. Numerous efforts were made to increase the longevity of current structures and create corrosion management techniques in an effort to lower the danger of corrosion. Since the most efficient inhibitors have conjugated π-bonds in their cyclic skeletons and rings with appropriate heteroatoms like O, S, and N, they are among the best methods for preventing steel corrosion, particularly in petroleum and chemical industries [20]. A corrosion inhibitor represents a material that prevents or inhibits corrosion in corrosive environments in the case when applied in trace levels [13]. The interaction between corrosive solution and metal surface could be limited by corrosion inhibitors, which might adsorb at metal-solution contact chemically and/or physically [21]. Certain inhibitors may be employed as antifungal, anti-inflammatory, and antibacterial agents [22, 23]. Through investigating its antibacterial, anti-corrosion, and antioxidant qualities, the presented work seeks to assess previously synthesized compound, 5-(4-nitrophenyl)-4-((4-phenoxy-benzylidene)amino)-4H-1,2,4-triazole -3thiol (NPAT) in Fig.1, which has the molecular weight (417.44 g/mol) and chemical formula ($C_{12}H_{15}N_5O_3S$) [24]. It is capable of offering complete protection in acidic media. The electrochemical impedance spectroscopy (EIS) and potentiodynamic polarization (PDP) have been used for evaluating corrosion resistance activity.

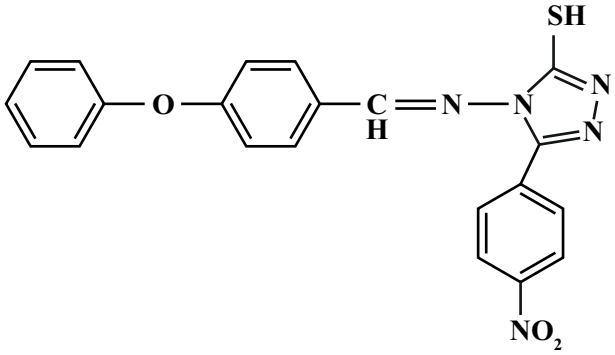

Fig. 1. Chemical structure of NPAT Schiff base compound

MATERIALS AND METHODS

Metal specimens

The working electrodes in the presented work have been carbon steel alloy (CS) with mass percentages of Fe 99.50, Mn 0.199, Si <0.0100, C 0.0855, Ni <0.0250, Cu 0.0260, Al 0.04410, Cr 0.0341, and other kinds of metals (0.096). CS were divided into small, 2.5 × 0.2 mm pieces. CS coupons were washed as well as degreased using acetone, ethanol, and distilled water after being abraded with emery papers (grade 400–1200) prior to testing.

Test solution

1M hydrochloric acid (HCl, 37 %, BDH Company) and the inhibitor NPAT Schiff base compound at concentrations of 15, 25, and 35 ppm were present in corrosive media.

Electrochemical testing

Charge transfer resistance, corrosion current density, and inhibition efficiency have been measured using EIS and PDP. The PDP was measured in the range −0.25 V to +0.25 V vs open circuit potential (OCP) with polarization rate 5 mV/s after 900 s of OCP stabilization. The EIS measurements were carried out over a frequency range of 0.1 Hz to 100 kHz using an AC perturbation amplitude of 10 mV, after 900 s of OCP stabilization. Three electrodes – a type cell consisting of CS as working electrode, platinum wire as counter electrode, and a silver/silver chloride electrode as reference electrode – had been used for electrochemical testing. IVIUM TECHNOLOGIES NETHERLANDS' Vertex One potentiostat/Galvanostat/EIS was utilized.

Antibacterial activity

With the use of gram positive (*S. aureus*) and gram negative (*E. coli*) bacteria strains, the *in vitro* antibacterial activity of synthesized compound has been evaluated at various doses. The disc diffusion approach has been used to assess anti-bacterial activity, and wells with a 6mm diameter have been created in agar plate. The bacterial dish was incubated at a temperature of 310 K for 24 hours. The inhibitory zone's diameter in millimeters (mm) was measured [25] .

Antioxidant activity

The 2,2-diphenyl-1-picrylhydrazyl (DPPH) assay has been utilized in order to measure the produced compound's in vitro antioxidant ability against free radicals [26]. DPPH (4 mg) has been dissolved in methanol for creating the DPPH stock solution (100 ml), which was then stored in volumetric flask covered with aluminum foil to keep light out. One milligram of the test compound was dissolved in ten milliliters of methanol to create a stock solution with a 100 ppm concentration. The additional concentrations (75, 50, 25, and 12.5 ppm) were after that obtained by diluting such stock solution. Ascorbic acid (vitamin C) was synthesized at comparable concentrations for comparison. One milliliter of the tested compound was added to one milliliter of DPPH solution for each concentration, and the mix has then been allowed to sit at room temperature for half an hour. Just DPPH solution was present in blank solution. A spectrophotometer was used for measuring each solution's absorbance (Abs) at 517 nm. The potential for scavenging DPPH radicals has been calculated using the next formula:

$$I\ \% = [(\text{Abs blank} - \text{Abs sample}) / \text{Abs blank}] \times 100$$

RESULTS AND DISCUSSION

Measurements of corrosion rate

The next parameters could be used for describing the electrochemical corrosion kinetics regarding any system: Corrosion potential (E_{corr}, mV), Corrosion current density (I_{corr}, mA.cm^{-2}) that had been obtained by Anodic and cathodic Tafel slopes (βa and βc, mV.dec^{-1}) respectively, Penetration loss or corrosion rate (PL, mm.y^{-1}) expressed as millimeters per year, Polarization resistance (R_p, Ω·cm²) inverse indicator of corrosion rate under small perturbations. Percentage inhibition efficiency (IE %), calculated as [27, 28]:

$$IE\ \% = \frac{I_{corr,blank} - I_{corr,inh.}}{I_{corr,blank}} \cdot 100\ \% \qquad (1)$$

in which, $I_{corr,blank}$ and $I_{corr,inh.}$ denote values of corrosion current density in inhibitor absence and presence, respectively.

The potentiodynamic polarization curves for CS specimens under investigation, both with and without different inhibitor concentration levels, immersed in 1 M HCl solution at 293–313 K are depicted in Figure 2.

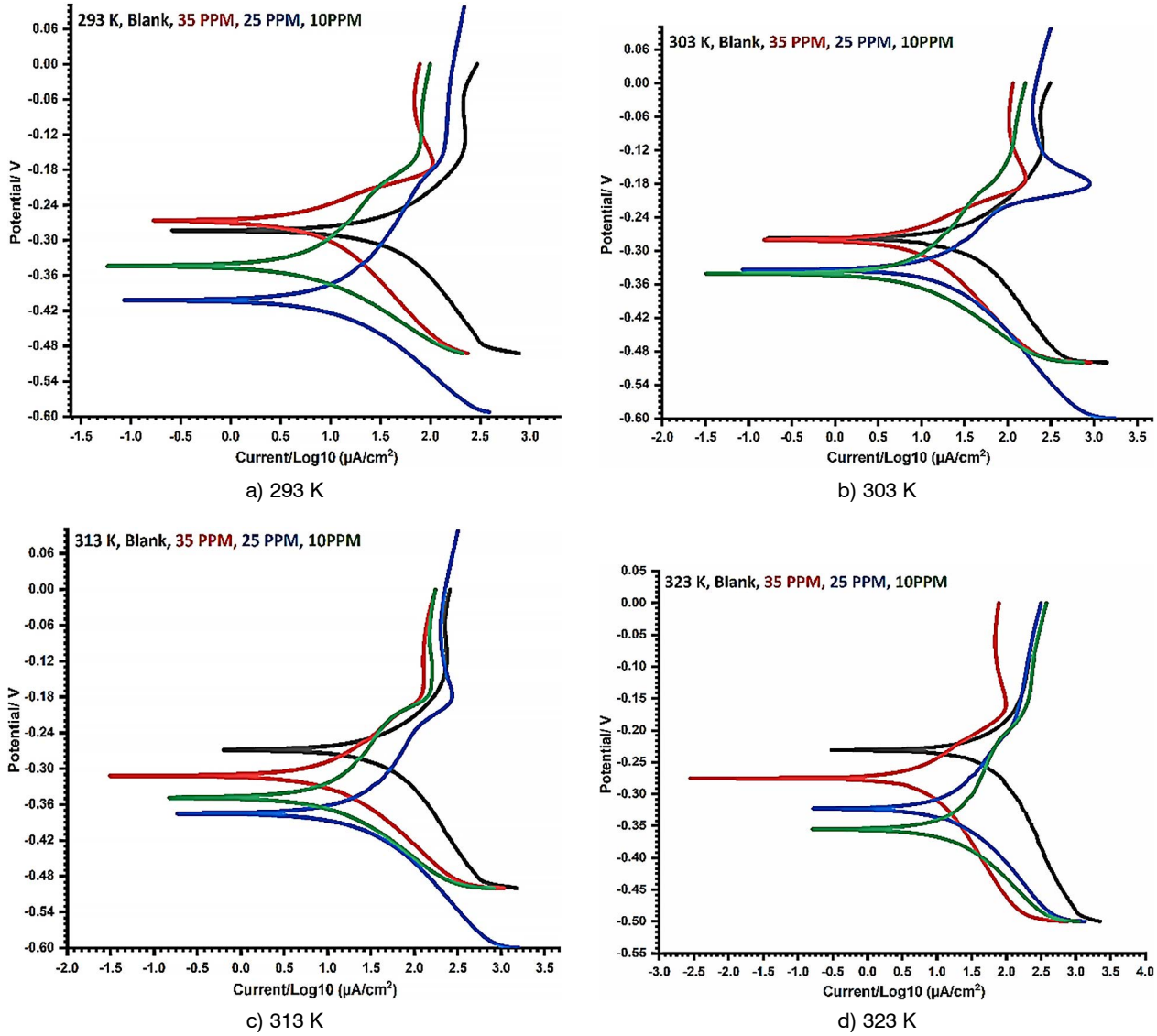

Fig. 2. Potentiodynamic polarization curves for CS in absence and presence of different concentration levels of inhibitor at 293–323 K

The electrochemical polarization parameters acquired for carbon steel corrosion in 1 M HCl solution at four temperature degrees (293–323 K) and with and without varying inhibitor doses (15, 25, and 35 ppm) are shown in Table 1. According to Table 1 data, corrosion current density (I_{corr}) gradually increases as temperature rises, suggesting that the corrosion process speeds up at higher temperatures. This behavior is explained by the higher rate regarding electrochemical reactions and the increased kinetic energy of corrosive species. As a result, it is confirmed that corrosion resistance deteriorates with temperature as corrosion rate (PL) increases and polarization resistance (R_p) drops. At all temperatures, I_{corr} is greatly decreased in case where inhibitor is added in comparison to blank solution. I_{corr} and corrosion rate significantly drop when inhibitor con-centration is increased from 15 to 35 ppm, whereas polarization resistance (R_p) increases concurrently. This pattern demonstrates that inhibitor molecules effectively adsorb onto carbon steel surface, creating a barrier that prevents metal dissolution as well as charge transfer. As the inhibitor concentration rises, inhibition efficiency (IE%) rises as well, peaking at 35 ppm. On the other hand, IE% falls as temperature rises for fixed inhibitor concentration. This decrease implies that inhibitor molecules partially desorb from metal surface at high temperature degrees, weakening the protective layer and mostly involving physical adsorption. The inhibitor functions as mixed-type inhibitor, as evidenced by comparatively slight variations in corrosion potential (E_{corr}) in its presence [29-31].

Tab. 1 Corrosion parameters and corresponding corrosion inhibition efficiency for CS corrosion in 1M HCl in absence and presence of different concentration levels of inhibitor at different temperaturesd

Systems	T (K)	$-E_{corr}$ (mV)	I_{corr} (mA/cm²)	βc (mV/dec)	βa (mV/dec)	PL (mm/y)	R_p (Ω/cm²)	IE %
Blank	293	277	0.07680	214	170	0.377	1072	–
	303	283	0.09114	224	197	0.447	998.0	–
	313	268	0.09639	206	170	0.473	839.6	–
	323	233	0.11340	203	164	0.556	694.7	–
35 ppm	293	339	0.01184	104	197	0.058	5002	84.58
	303	341	0.01474	102	179	0.072	3831	83.82
	313	312	0.01828	112	122	0.090	2775	81.03
	323	356	0.03568	104	216	0.175	1710	68.53
25 ppm	293	266	0.01534	173	126	0.075	4133	80.02
	303	276	0.01968	164	116	0.092	3003	78.40
	313	342	0.02318	113	201	0.114	2712	75.94
	323	321	0.04349	130	188	0.213	1538	61.64
15 ppm	293	390	0.02218	136	202	0.109	3191	71.11
	303	333	0.04019	168	177	0.197	1860	55.90
	313	376	0.04385	127	205	0.215	1557	54.50
	323	277	0.06034	235	156	0.296	1351	46.79

EIS studies

EIS was used to determine a wide range of frequencies for determining how the corroding alloy responds to small-amplitude alternating potential signals. At high frequency values, EIS has been a complicated combination of interface capacitance, charge transfer resistance, mass transfer capacitance, and solution resistance. The Nyquist and Bode EIS plots and the fitted curve for CS corrosion in acidic media at different inhibitor concentration levels are displayed in Figures 3 and 4. Figure 5 displays the recommended equivalent circuit for acquired Nyquist plot. It is made up of a double layer capacitor (CPE(dl), a charge transfer resistance (R_p), and a solution resistance (R_s). R_p and CPE (dl) are in parallel. Table 2 lists the components utilized in the corresponding circuit (Fig. 5). The roughness and inhomogeneity of CS surface are responsible for the divergence from conventional semicircle seen non all of the Nyquist spectra (Fig. 3) [32]. When an inhibitor is added, the Nyquist plots' semicircle's diameter increases without changing the plot's shape. This implies that adsorption related to inhibitor molecules on CS surface, independent of changes in the corrosion mechanism, is the cause of NPAT's inhibitory activity [33]. The adsorption related to a film of NPAT molecules on CS surface is confirmed by the addition of an inhibitor, which widens the phase angle maxima (Fig. 4) at intermediate frequency [34]. The next relationship [35] was used for further validating the corrosion inhibition efficiency (IE %) of NPAT inhibitor utilizing EIS data:

$$IE\ \% = \frac{R_{p\,(\text{inh.})} - R_{p\,(\text{blank})}}{R_{p\,(\text{inh.})}} \cdot 100\ \% \qquad (2)$$

where R_p (blank) and R_p (inh.) charge transfer resistance values without and with NPAT inhibitor, respectively.

Table 2 displays the determined IE % values. Examining the results (Tab. 2) reveals that as concentrations rise, so does the inhibitor's ability to inhibit. The EIS parameters show that the inhibitor's presence has a major impact on carbon steel's electrochemical response. In comparison to 25 ppm and 15 ppm, R_p is maximum at all temperatures at 35 ppm. It also exhibits a significant IE% (~55.37 %), suggesting severe inhibition at low temperatures. IE % falls with T for constant inhibitor concentration because the percentage rise in R_p brought on by the inhibitor lowers with temperature. Because physical adsorption regarding inhibitor compounds is less thermally durable compared to chemical adsorption, such pattern suggests that the protective film diminishes at higher temperatures. Surface coverage as well as film heterogeneity resulting from inhibitor adsorption are further supported by non-ideal double-layer response indicated in CPE variations. Increased surface coverage is confirmed by higher R_p values at higher inhibitor concentrations, raising the energy barrier for electron transfer at metal/solution interface. The concentration of 35 ppm produced the highest IE % value, which was 55.37 %. The IE percentage values are in agreement with potentiodynamic polarization study data (Tab. 1) [36].

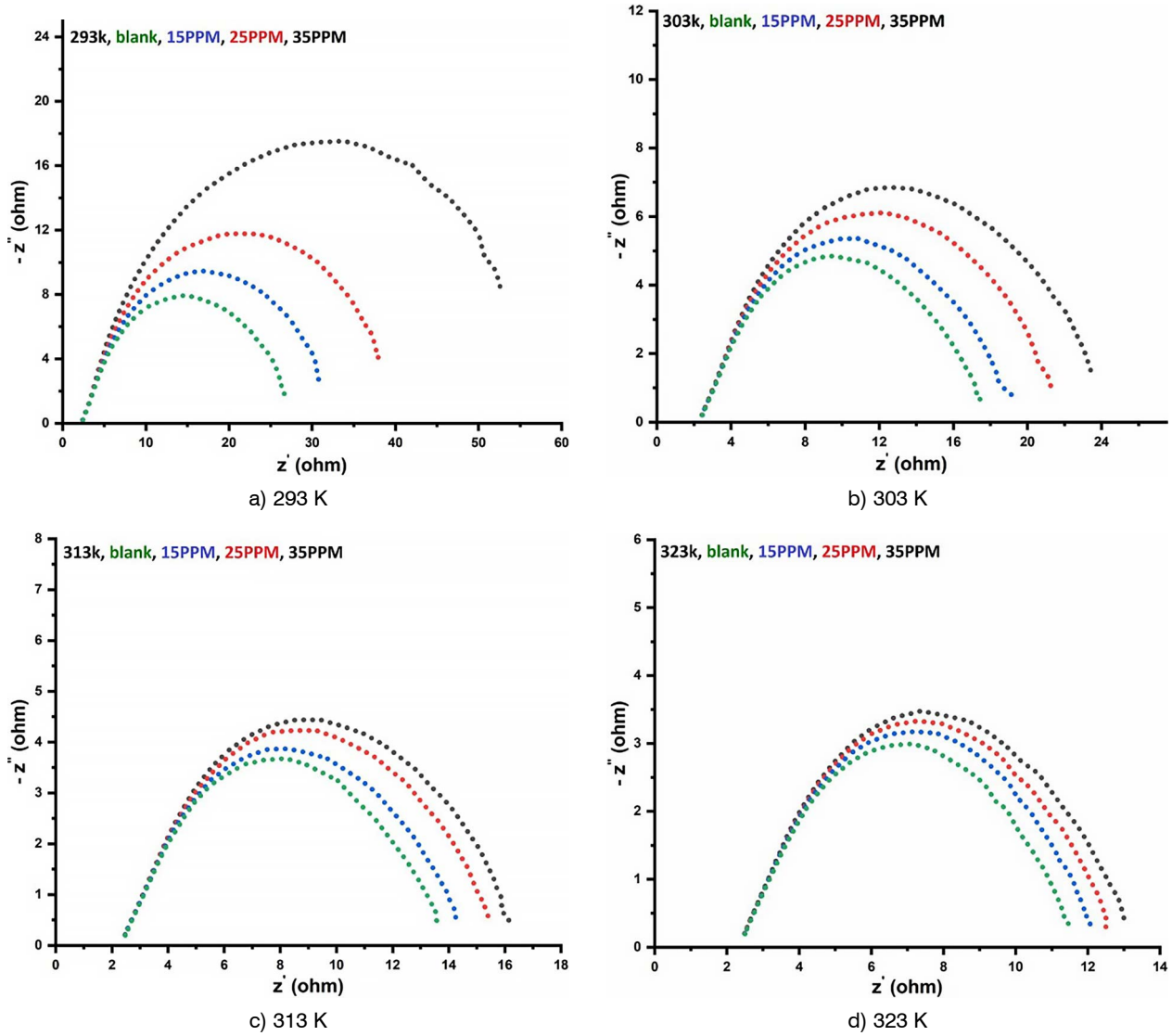

a) 293 K b) 303 K

c) 313 K d) 323 K

Fig. 3. Nyquist plots of CS in 1M HCl with and without various concentration levels of NPAT at 293–323 K

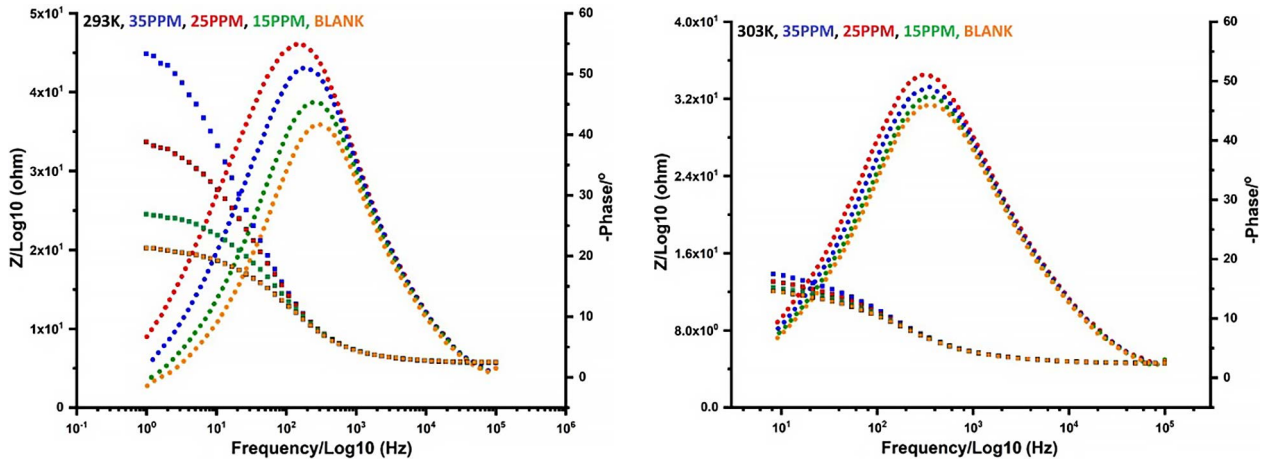

a) 293 K b) 303 K

Fig. 4. Bode plots of CS in 1M HCl with and without various concentration levels of NPAT at 293–323 K *(continue on next page)*

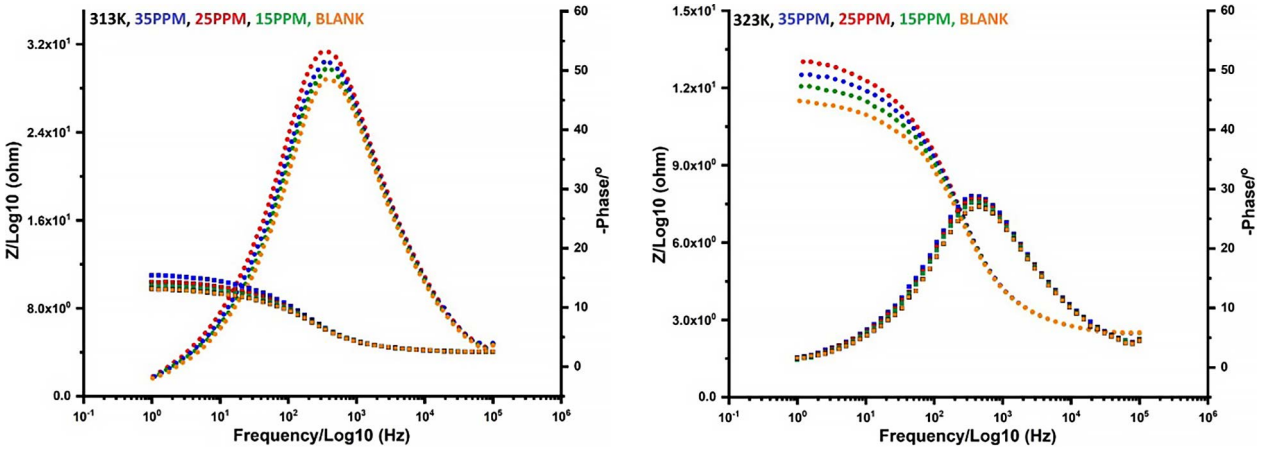

c) 313 K d) 323 K

Fig. 4. Bode plots of CS in 1M HCl with and without various concentration levels of NPAT at 293–323 K

Tab. 2 EIS parameters and corresponding efficiency of corrosion inhibition for corrosion of CS in 1M HCl in absence and presence of various concentration levels of inhibitor at different temperatures

System	T (K)	R_s (Ω)	R_p (Ω)	$CPE_{(dl)}$ (μF)	IE (%)
Blank (CS)	293	2.405	25.440	721.1	–
	303	2.420	15.280	741.6	–
	313	2.441	11.350	756.6	–
	323	2.754	7.192	775.3	–
35 ppm	293	2.349	57.000	804.8	55.37
	303	2.406	21.860	719.5	30.10
	313	2.432	14.488	732.7	21.66
	323	2.805	10.163	721.6	17.89
25 ppm	293	2.384	38.460	735.9	33.85
	303	2.419	19.360	715.5	21.07
	313	2.427	13.230	740.9	14.21
	323	2.450	8.230	750.1	12.61
15 ppm	293	2.400	30.370	716.0	16.23
	303	2.417	16.810	724.0	9.10
	313	2.433	12.080	753.9	6.04
	323	2.458	7.536	748.0	4.57

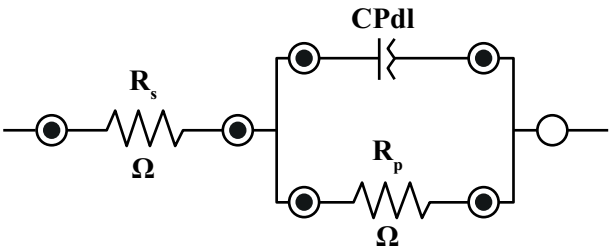

Fig. 5. Equivalent circuit of CS

Adsorption isotherm

The adsorption isotherm could be used to characterize the type of interactions that occur between CS surface as well as NPAT molecules throughout the process of corrosion inhibition. In this instance, the present work is described using Freundlich isotherm (Eq. 3) [37, 38].

$$\text{Log}\,(\theta) = \text{Log}\,K_f + \frac{1}{n}\,\text{Log}\,C_{\text{inh.}} \tag{3}$$

were K_F represents Freundlich constant, $(1/n)$ is the Freundlich slope $(1/n)$, (Θ = IE%/100 by EIS method) and $C_{\text{inh.}}$ represents inhibitor concentration. Given the high likelihood of multilayer adsorption creation over the heterogeneous surface, we used Freundlich isotherm to characterize such situation.

Figure 6 and Table 3 display Freundlich adsorption isotherm plots as well as parameters, respectively. The fitting of the adsorption data to Freundlich isotherm is confirmed by the graphs in Figure 6, which show

crucial linearity with R^2 values close to one [39, 40]. The favorable adsorption conditions are confirmed by the ($1/n$) values given in Table 3 [41]. We may determine Gibb's free energy of the process of adsorption by using Eq. 4 [42-44].

$$\Delta G^{o}_{ads.} = RT \ln (55.5\ K_f) \quad (4)$$

in this case, T represents absolute temperature and R represents molar gas constant. Since Gibb's free energy for adsorption is (−20 KJ) for the physical adsorption process (Tab. 4), data showed that the adsorption regarding NPAT molecules on CS surface is spontaneous and of physical nature [45, 46].

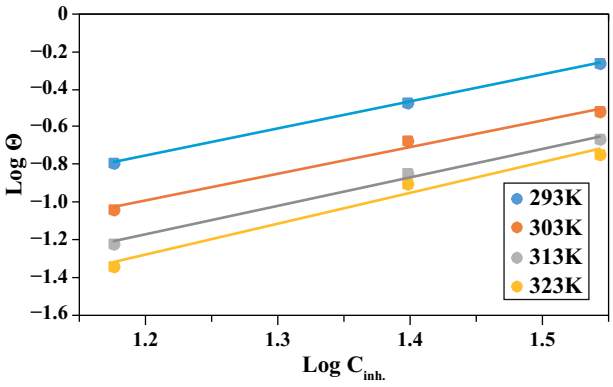

Fig. 6. Freundlich isotherm plots for NPAT adsorption on CS surface

Tab. 3 Adsorption isotherm parameters obtained from the EIS data for Cs in 1M HCl in presence of NPAT at different temperatures

T (K)	R^2	$1/n$	$-K_F$ (M^{-1})	ΔG^{o}_{ads} (kJ.mol^{-1})
293	1.0000	1.4476	2.4927	−12.0089
303	0.9878	1.4307	2.7102	−12.6295
313	0.9943	1.5209	2.9979	−13.3088
323	0.9754	1.6389	3.2457	−13.9473

Antibacterial activity

Two bacterial isolates (*E. coli* and *S. aureus*) had been used in order to test the antibacterial activity regarding various concentrations of the synthesized compound (75, 50, 25, and 12.5 ppm). The impact of varying tested compound concentrations on the bacterial isolates was displayed in Table 4 as the diameter regarding the inhibition zone (mm). The compound that was tested had the greatest effect on *S. aureus* (25 mm) at the highest concentration (75 ppm).

Tab. 4 The Antibacterial activity of produced compound

Compound concentration (ppm)	Inhibition zone (mm)	
	Staphylococcus aureus	Escherichia coli
75	25	18
50	20	15
25	16	10
12.5	8	–

Antioxidant activity

With the use of DPPH radical scavenging assay, the antioxidant activity regarding the produced compound has been assessed in vitro at various concentrations (100, 75, 50, 25, and 12.5 ppm), yielding an IC50 of (94.36). Comparing the studied compound to ascorbic acid, Table 5 indicates that it had the highest DPPH radical scavenging activity at 100 ppm. In comparison to DPPH, the compound showed moderate antioxidant activity at 100 ppm.

Tab. 5 The radical scavenging activity (%) of produced compound

Concentration (ppm)	Inhibition (%)	
	Tested compound	Ascorbic acid
100	54.8	95.76
75	36.6	80.2
50	23.4	55.6
25	11.3	28.17
12.5	3.0	13.99

CONCLUSION

The newly compound is a promising environmentally friendly inhibitor for industrial uses in acidic conditions since it has good anticorrosion, moderate antibacterial, and antioxidant qualities. It is advised that more research be done on long-term stability as well as environmental safety.

REFERENCES

1. K.A. Abdelshafeek,A. El-Shamy, Review on glucosinolates: Unveiling their potential applications as drug discovery leads in extraction, isolation, biosynthesis, biological activity, and corrosion protection, *Food Bioscience,* **2023**, 56, 103071, DOI: 10.1016/j.fbio.2023.103071
2. R.M. Nasser,N.M. Masmali, The effectiveness of Tamarindus Indica extracts as a metal corrosion inhibitor in various circumstances, *Anti-Corrosion Methods and Materials,* **2022**, 69, 224-233, DOI: 10.1108/ACMM-06-2021-2490
3. A. Sedik, D. Lerari, A. Salci, S. Athmani, K. Bachari, İ. Gecibesler, R. Solmaz, Dardagan Fruit extract as eco-friendly corrosion inhibitor for mild steel in 1 M HCl: Electrochemical and surface morphological studies, *Journal of the Taiwan Institute of Chemical Engineers,* **2020**, 107, 189-200, DOI: 10.1016/j.jtice.2019.12.006

4. M. Shehata,A. El-Shamy, Hydrogen-based failure in oil and gas pipelines a review, *Gas Science and Engineering,* **2023**, 115, 204994, DOI: 10.1016/j.jgsce.2023.204994
5. X. Wang, L. Chen, F. Yang, Q. Xiang, J. Liu, Corrosion inhibition mechanism and extraction technology of plant corrosion inhibitors: a review, *Journal of Adhesion Science and Technology,* **2023**, 37, 2919-2943, DOI: 10.1080/01694243.2023.2172993
6. A.M. Abdel-Karim,A.M. El-Shamy, A review on green corrosion inhibitors for protection of archeological metal artifacts, *Journal of Bio-and Tribo-Corrosion,* **2022**, 8, 35, DOI: 10.1007/s40735-022-00636-6
7. A. Okewale,F. Omoruwuo, Neem leaf extract as a corrosion inhibitor on mild steel in acidic solution, *International Journal of Engineering Research in Africa,* **2018**, 35, 208-220, DOI: 10.4028/www.scientific.net/JERA.35.208
8. J. Panchal, D. Shah, R. Patel, S. Shah, M. Prajapati, M. Shah, Comprehensive review and critical data analysis on corrosion and emphasizing on green eco-friendly corrosion inhibitors for oil and gas industries, *Journal of Bio-and Tribo-Corrosion,* **2021**, 7, 107, DOI: 10.1007/s40735-021-00540-5
9. M. Alimohammadi, M. Ghaderi, A. Ramazani SA, M. Mahdavian, Falcaria vulgaris leaves extract as an eco-friendly corrosion inhibitor for mild steel in hydrochloric acid media, *Scientific Reports,* **2023**, 13, 3737, DOI: 10.1038/s41598-023-30571-6
10. D.T. Oyekunle, T.I. Oguntade, C.S. Ita, T. Ojo, O.D. Orodu, Corrosion inhibition of mild steel using binary mixture of sesame and castor oil in brine solution, *Materials Today Communications,* **2019**, 21, 100691, DOI: 10.1016/j.mtcomm.2019.100691
11. K. Rashid,A. Khadom, Evaluation of environmentally friendly inhibitor for corrosion of mild steel in phosphoric acid solution: unconventional approach, *Anti-corrosion methods and materials,* **2018**, 65, 506-514, DOI: 10.1108/ACMM-06-2018-1955
12. Y. Sasikumar, A. Adekunle, L.O. Olasunkanmi, I. Bahadur, R. Baskar, M.M. Kabanda, I. Obot, E.E. Ebenso, Experimental, quantum chemical and Monte Carlo simulation studies on the corrosion inhibition of some alkyl imidazolium ionic liquids containing tetrafluoroborate anion on mild steel in acidic medium, *Journal of Molecular Liquids,* **2015**, 211, 105-118, DOI: 10.1016/j.molliq.2015.06.052
13. W. Ahmaeed, A. Abd, A. Khadom, Corrosion inhibition effect of sodium iodide for mild steel in 1 M hydrochloric acid: Gravimetrical and electrochemical studies, *International Journal of Corrosion and Scale Inhibition,* **2019**, 8, 1097-1111, DOI: 10.17675/2305-6894-2019-8-4-17
14. K. Boumhara, H. Harhar, M. Tabyaoui, A. Bellaouchou, A. Guenbour, A. Zarrouk, Corrosion inhibition of mild steel in 0.5 M H_2SO_4 solution by Artemisia herba-alba oil, *Journal of Bio-and Tribo-Corrosion,* **2019**, 5, 8, DOI: 10.1007/s40735-018-0202-8
15. J. Kaur, N. Daksh, A. Saxena, Corrosion inhibition applications of natural and eco-friendly corrosion inhibitors on steel in the acidic environment: an overview, *Arabian Journal for Science and Engineering,* **2022**, 47, 57-74, DOI: 10.1007/s13369-021-05699-0
16. B. TK, J. C, A. P, Corrosion inhibition of mild steel in hydrochloric acid by leaves extract of Tephrosia purpurea, *Journal of Adhesion Science and Technology,* **2020**, 34, 2424-2447, DOI: 10.1080/01694243.2020.1766395
17. W.M.I.W.M. Kamaruzzaman, N.A.M. Nasir, N.A.S.M. Hamidi, N. Yusof, M.S. Shaifudin, A.M.A.A.M. Suhaimi, M.A. Badruddin, A. Adnan, W.M.N.W. Nik, M.S.M. Ghazali, 25 years of progress on plants as corrosion inhibitors through a bibliometric analysis using the Scopus database (1995–2020), *Arabian journal of Chemistry,* **2022**, 15, 103655, DOI: 10.1016/j.arabjc.2021.103655
18. H. Hamani, T. Douadi, D. Daoud, M. Al-Noaimi, R.A. Rikkouh, S. Chafaa, 1-(4-Nitrophenylo-imino)-1-(phenylhydrazono)-propan-2-one as corrosion inhibitor for mild steel in 1 M HCl solution: weight loss, electrochemical, thermodynamic and quantum chemical studies, *Journal of Electroanalytical Chemistry,* **2017**, 801, 425-438, DOI: 10.1016/j.jelechem.2017.08.031
19. A.H. Radhi, E.A. Du, F.A. Khazaal, Z.M. Abbas, O.H. Aljelawi, S.D. Hamadan, H.A. Almashhadani, M.M. Kadhim, HOMO-LUMO energies and geometrical structures effecton corrosion inhibition for organic compounds predict by DFT and PM3 methods, *NeuroQuantology,* **2020**, 18, 37-45, DOI: 10.14704/nq.2020.18.1.NQ20105
20. K. Cherrak, M. El Massaoudi, H. Outada, M. Taleb, H. Lgaz, A. Zarrouk, S. Radi, A. Dafali, Electrochemical and theoretical performance of new synthetized pyrazole derivatives as promising corrosion inhibitors for mild steel in acid environment: Molecular structure effect on efficiency, *Journal of Molecular Liquids,* **2021**, 342, 117507, DOI: 10.1016/j.molliq.2021.117507
21. M. Pramudita, S. Sukirno, M. Nasikin, Synergistic corrosion inhibition effect of rice husk extract and KI for mild steel in H_2SO_4 solution, *Bulletin of Chemical Reaction Engineering & Catalysis,* **2019**, 14, 697-704, DOI: 10.9767/bcrec.14.3.4249.697-704
22. F.Z. Fan ZhiJiang, S.J. Shi Jun, L.N. Luo Na, D.M. Ding MuHan, B.X. Bao XiaoPing, Synthesis, crystal structure, and agricultural antimicrobial evaluation of novel quinazoline thioether derivatives incorporating the 1, 2, 4-triazolo 4, 3-a] pyridine moiety, **2019**, DOI: 10.1021/acs.jafc.9b04733
23. O. Ibrahim, E. Bakhite, S. Metwally, Y. El-Ossaily, H. Abdu-Allah, E. Al-Taifi, M. Kandel, Synthesis, characterization, and antifungal activity of some new thieno 2, 3-b] pyridines incorporating quinazoline or benzimidazole moiety, *Russian Journal of Bioorganic Chemistry,* **2021**, 47, 918-928, DOI: 10.1134/S1068162021040117
24. A.T. Bader, N.A.R. Al-qasii, A.H. Shntaif, M. El Marouani, M.I.H.A. Majidi, L. Trif, M. Boulhaoua, Synthesis, structural analysis and thermal behavior of new 1, 2, 4-triazole derivative and its transition metal complexes, *Indonesian Journal of Chemistry,* **2022**, 22, 223-232, DOI: 10.22146/ijc.68859
25. E.M. Hussain, Synthesis and antibacterial evaluation for some new schiff-bases derived from P-aminoacetanilide, *Baghdad Science Journal,* **2023**, 20, 2455-2455, DOI: 10.21123/bsj.2023.8905
26. R.S. Dawood,F.N. Faisal, The use of the carbonyl group (C-3) of Isatin for the construction of pyrazoline moiety and the study of its antioxidant activity, *Iraqi Journal of Science,* **2024**, 5395-5405, DOI: 10.21123/bsj.2023.8905
27. B. Xue, Y. Jiang, D. Liu, Preparation and characterization of a novel anticorrosion material: Cu/LLDPE nanocomposites, *Materials transactions,* **2011**, 52, 96-101, DOI: 10.2320/matertrans.M2010280

28. R.W. Revie, Uhlig's corrosion handbook, *Journal,* **2011**, DOI: 10.1002/9780470872864
29. S. Alaoui Mrani, E. Ech-Chihbi, N. Arrousse, Z. Rais, F. El Hajjaji, C. El Abiad, S. Radi, J. Mabrouki, M. Taleb, S. Jodeh, DFT and electrochemical investigations on the corrosion inhibition of mild steel by novel Schiff's base derivatives in 1 M HCl solution, *Arabian Journal for Science and Engineering,* **2021**, 46, 5691-5707, DOI: 10.1007/s13369-020-05229-4
30. E.K. Ardakani, E. Kowsari, A. Ehsani, Imidazolium-derived polymeric ionic liquid as a green inhibitor for corrosion inhibition of mild steel in 1.0 M HCl: Experimental and computational study, *Colloids and Surfaces A: Physicochemical and Engineering Aspects,* **2020**, 586, 124195, DOI: 10.1016/j.colsurfa.2019.124195
31. A. Zarrouk, B. Hammouti, T. Lakhlifi, M. Traisnel, H. Vezin, F. Bentiss, New 1H-pyrrole-2, 5-dione derivatives as efficient organic inhibitors of carbon steel corrosion in hydrochloric acid medium: electrochemical, XPS and DFT studies, *Corrosion Science,* **2015**, 90, 572-584, DOI: 10.1016/j.corsci.2014.10.052
32. M. Deyab, Effect of carbon nano-tubes on the corrosion resistance of alkyd coating immersed in sodium chloride solution, *Progress in Organic Coatings,* **2015**, 85, 146-150, DOI: 10.1016/j.porgcoat.2015.04.003
33. K.W. Tan, M.J. Kassim, C.W. Oo, Possible improvement of catechin as corrosion inhibitor in acidic medium, *Corrosion science,* **2012**, 65, 152-162, DOI: 10.1016/j.corsci.2012.08.012
34. S. John,A. Joseph, Electro analytical, surface morphological and theoretical studies on the corrosion inhibition behavior of different 1, 2, 4-triazole precursors on mild steel in 1 M hydrochloric acid, *Materials Chemistry and Physics,* **2012**, 133, 1083-1091, DOI: 10.1016/j.matchemphys.2012.02.020
35. M. Deyab, K. Eddahaoui, R. Essehli, S. Benmokhtar, T. Rhadfi, A. De Riccardis, G. Mele, Influence of newly synthesized titanium phosphates on the corrosion protection properties of alkyd coating, *Journal of Molecular Liquids,* **2016**, 216, 699-703, DOI: 10.1016/j.molliq.2016.01.092
36. A. Dehghani, G. Bahlakeh, B. Ramezanzadeh, M. Ramezanzadeh, Potential role of a novel green eco-friendly inhibitor in corrosion inhibition of mild steel in HCl solution: Detailed macro/micro-scale experimental and computational explorations, *Construction and Building Materials,* **2020**, 245, 118464, DOI: 10.1016/j.conbuildmat.2020.118464
37. M. Deyab, R. Essehli, B. El Bali, Performance evaluation of phosphite NaCo $(H_2PO_3)_3 \cdot H_2O$ as a corrosion inhibitor for aluminum in engine coolant solutions, *RSC Advances,* **2015**, 5, 48868-48874, DOI: 10.1039/C5RA06611E
38. E. Ituen, A. James, O. Akaranta, Fluvoxamine-based corrosion inhibitors for J55 steel in aggressive oil and gas well treatment fluids, *Egyptian journal of petroleum,* **2017**, 26, 745-756, DOI: 10.1016/j.ejpe.2016.10.002
39. D. Karadag, Y. Koc, M. Turan, M. Ozturk, A comparative study of linear and non-linear regression analysis for ammonium exchange by clinoptilolite zeolite, *Journal of hazardous materials,* **2007**, 144, 432-437, DOI: 10.1016/j.jhazmat.2006.10.055
40. D.E. AL-Mammar,R.A. Mohammed, Study the adsorption of basic violet 10 dye onto olive kernels powder as adsorbent in aqueous solution, *Iraqi Journal of Science,* **2025**, 2188-2202, DOI: 10.24996/ijs.2025.66.6.2
41. M. Deyab, Electrochemical investigations on pitting corrosion inhibition of mild steel by provitamin B5 in circulating cooling water, *Electrochimica Acta,* **2016**, 202, 262-268, DOI: 10.1016/j.electacta.2015.11.075
42. E. Bayol, A. Gürten, M. Dursun, K. Kayakirilmaz, Adsorption behavior and inhibition corrosion effect of sodium carboxymethyl cellulose on mild steel in acidic medium, *Acta Physico-Chimica Sinica,* **2008**, 24, 2236-2243, DOI: 10.1016/S1872-1508(08)60085-6
43. G. Avci, Inhibitor effect of N, N′-methylenediacrylamide on corrosion behavior of mild steel in 0.5 M HCl, *Materials Chemistry and Physics,* **2008**, 112, 234-238, DOI: 10.1016/j.matchemphys.2008.05.036
44. M. Lebrini, F. Robert, H. Vezin, C. Roos, Electrochemical and quantum chemical studies of some indole derivatives as corrosion inhibitors for C38 steel in molar hydrochloric acid, *Corrosion Science,* **2010**, 52, 3367-3376, DOI: 10.1016/j.corsci.2010.06.009
45. O. Abiola,N. Oforka, Adsorption of (4-amino-2-methyl-5-pyrimidinyl methylthio) acetic acid on mild steel from hydrochloric acid solution (HCl) – Part 1, *Materials Chemistry and Physics,* **2004**, 83, 315-322, DOI: 10.1016/j.matchemphys.2003.10.001
46. B.D. Mert, M.E. Mert, G. Kardaş, B. Yazıcı, Experimental and theoretical investigation of 3-amino-1, 2, 4-triazole-5-thiol as a corrosion inhibitor for carbon steel in HCl medium, *Corrosion science,* **2011**, 53, 4265-4272, DOI: 10.1016/j.corsci.2011.08.038